Journal of ELECTRICAL ENGINEERING, VOL. 64, NO. 4, 2013, 201–211

PERFORMANCE OF CONVERTERS SUITABLE FOR SWITCHED RELUCTANCE GENERATOR (SRG) OPERATION

Valéria Hrabovcová * — **Pavol Rafajdus** *
Martin Lipták ** — **Loránd Szabó** ***

The paper deals with various kinds of converter topologies and their performances suitable for SRG operation. For each topology the equivalent circuit, mathematical model and simulation waveforms of phase variables are given. At the end of the paper the performances of individual converter topologies are compared and recommendations for their employment are given.

K e y w o r d s: switched reluctance generator, converter, mathematical model, simulation

1 INTRODUCTION

Switched reluctance (SR) machines belong to the machines which are obviously called electronically commutated machines. It means that they are not able to operate on the rigid grid with a constant voltage and frequency, but they need to cooperate with converters. Therefore it is very important to investigate how a converter topology influences the performances of this machine operation [1].

At present various kinds of converter topologies are known for switched reluctance motor (SRM) operation. Many of them are described in [2–4], but not all are suitable for switched reluctance generator (SRG) operation. In this paper detailed analyses of those, which are suitable for the SRG operation are given.

As it is known, a motoring torque is developed during the period of inductance increasing and generating torque during the period of inductance decreasing. However during the generating period in a generator operation there are defined excitation and generation periods. The excitation period is between the $\theta_{\rm on}$ and $\theta_{\rm off}$ in Fig. 1, during which the phase is excited from a dc source (or from a capacitor), or in the next cycle the generated energy of the SRG is utilized for its own excitation. Then there is a generation period, between $\theta_{\rm off}$ and $\theta_{\rm ext}$, during which electrical energy is generated and delivered to the load [5]. As it can be seen in Fig. 2, the values of $\theta_{\rm on}$ and $\theta_{\rm off}$ are very important variables affecting output parameters of the SRG.

The converters employed for SR machines are obviously divided according the number of switches, usually transistors, per phase. If the phase number is m, then there are converters with *eg* m, $m+1$, $1.5m$, $2m$ switches. However there are more details which can be important for the converter's evaluation, and then converters can be called as: converter with neutral point of the source, converter with a capacitor, converter with bifilar winding, and converter with controlled dc bus voltage. All these converters are suitable for the SRG operation,

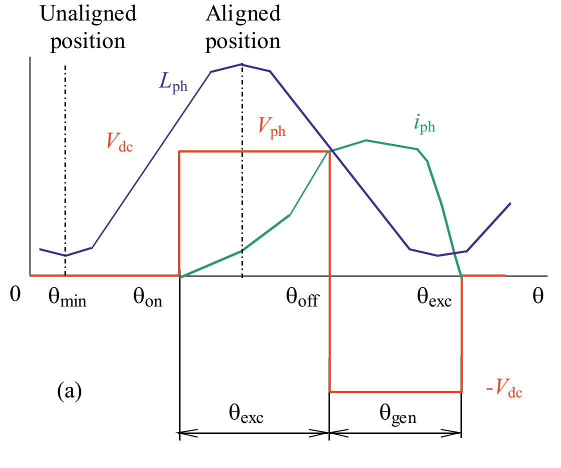

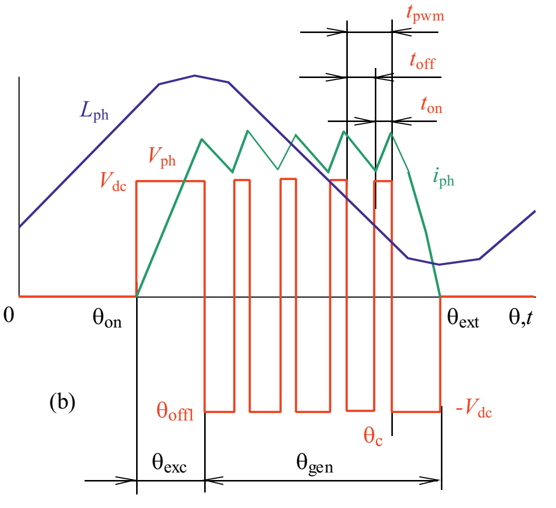

Fig. 1. SRG phase variables at a) – single pulse operation, b) – multi-pulse operation, current control

* University of Žilina, Faculty of Electrical Engineering, Slovakia, pavol.rafajdus@fel.uniza.sk, valeria.hrabovcova@fel.uniza.sk
** Treves s.r.o., 17. listopadu 341, 544 01 Dvůr Králové nad Labem, Czech Republic, *** Technical University of Cluj-Napoca, Department of Electrical Machines and Drives, Romania

DOI: 10.2478/jee-2013-0030, Printed ISSN 1335-3632, On-line ISSN 1339-309X, © 2013 FEI STU

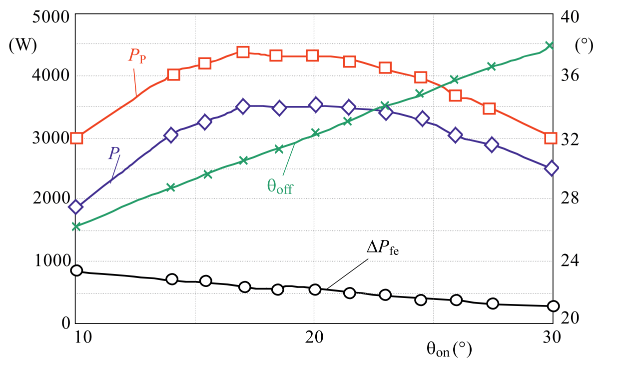

Fig. 2. Input power, output power, iron losses and $\theta_{\rm off}$ *vs* $\theta_{\rm on}$

will be analyzed in greater details and their performances will be compared.

2 MATHEMATICAL MODELS AND SIMULATION WAVEFORMS

2.1 Mathematical model of the $2m$ converter (C2m)

As it will be seen below, the $2m$ converter gives most favorite performances, the equivalent circuit in single and three phase configuration of which is shown in Fig. 3. To present how the procedure of the simulation will be carried out, this converter is analyzed in greater details.

The equivalent circuit is a base for a mathematical model, needed for simulation. In Fig. 3a there are seven unknown variables for which seven equations have to be written. Four of them, for current and voltage phase values, must be written extra for each phase

$$\frac{\mathrm{d}i_{ph}}{\mathrm{d}t} = \frac{1}{L_{ph}}\Big[v_{ph} - \Big(R_{ph} + \frac{\mathrm{d}L_{ph}}{\mathrm{d}\theta}\omega\Big)i_{ph}\Big], \tag{1}$$

$$i_{\rm in} = \begin{cases} i_{ph}\,, & \text{if S1 and S2 are switched on,} \\ 0 & \text{at least one of S1, S2 is switched off.} \end{cases} \tag{2}$$

$$i_{\rm out} = \begin{cases} i_{ph}\,, & \text{if S1 and S2 are switched off,} \\ 0\,, & \text{at least one of S1, S2 is switched on.} \end{cases} \tag{3}$$

$$v_{ph} = \begin{cases} +v_{dc}\,, & \text{if S1 and S2 are switched on,} \\ -v_{dc}\,, & \text{if S1 and S2 are switched off,} \\ 0\,, & \text{if only one of S1, S2} \\ & \text{is switched on or } i_{ph}=0\,, \end{cases} \tag{4}$$

where $i_{\rm in}$ is a total current during the period of excitation, and $i_{\rm out}$ is a total current during the period of generation.

The further three equations are common for all phases or better to say for the whole generator, and are for capacitor current $i_{\rm c}$, load current $i_{\rm L}$ and dc voltage $v_{\rm dc}$.

$$i_c = \sum_{j=1}^{m} i_{{\rm out}\,j} - \sum_{j=1}^{m} i_{{\rm in}\,j} - i_{\rm L}\,, \tag{5}$$

$$i_{\rm L} = \frac{v_{\rm dc}}{R_{\rm L}}\,, \tag{6}$$

$$\frac{\mathrm{d}v_{\rm dc}}{\mathrm{d}t} = \frac{1}{C}i_{\rm c}\,. \tag{7}$$

The definitions of $i_{\rm in}$ and $i_{\rm out}$ are seen in Fig. 4 and in (8) and (9).

$$I_{\rm in} = \frac{1}{\theta_T}\int_{\theta_{\rm on}}^{\theta_{\rm off}} i_{ph}\mathrm{d}\theta\,, \tag{8}$$

$$I_{\rm out} = \frac{1}{\theta_T}\int_{\theta_{\rm off}}^{\theta_{\rm ext}} i_{ph}\mathrm{d}\theta\,, \tag{9}$$

$$\varepsilon = \frac{I_{\rm in}}{I_{\rm out}}\,, \tag{10}$$

$$P_{\rm out} = m(I_{\rm out} - I_{\rm in})\,V_{dc}\,. \tag{11}$$

By means of $i_{\rm in}$ and $i_{\rm out}$ two important parameters (see (10) and 11)) which will be evaluated for all converters, are defined. The first is an excitation factor ε and the second power output $P_{\rm out}$. It is seen that excitation factor should be as small as possible by small value of $I_{\rm in}$ and big value of $I_{\rm out}$. Besides, the big difference between them will give higher value of output power. Therefore both values are important for the converter evaluation. Before simulation waveforms and the results will be given, the control strategy, how to get a required torque and power, will be explained.

2.2 Simulation waveforms of the $2m$ converter (C2m)

The mathematical model from Section 2.1 was applied and a block diagram (see Fig. 5) for SRG simulation was created. The simulations were done for a SRG, which was originally manufactured as a SR motor with the followed rating: 3.7 kW, 3 000 rpm, 540 V. The input static parameters of all SRG mathematical models are obtained by means of FEM and they are verified by measurements. In greater details it can be found in [6, 7] and the basic SRG parameters are as follows: $L_{\rm max} = 40$ mH, $L_{\rm min} = 5.5$ mH, $R_{ph} = 0.7\,\Omega$.

Input parameters for single-pulse operation are $V_{\rm dc}$, ω and $\theta_{\rm off}$. The angle $\theta_{\rm on}$ is generated by PI regulator, which compares the required and real value of the dc voltage. If the power on the load $p_{\rm out\_L}$ and output power $p_{\rm out}$ is equal, the $v_{\rm dc}$ is constant and generator is in steady state condition. In Fig. 6 it is seen that the output power can be the same at various values of excitation parameters. In general, the power increases with increasing of the excitation period θexc = θoff − θon, but only to a specific value corresponding to the RMS current limit. In Fig. 7 there is seen excitation period and phase current *vs*

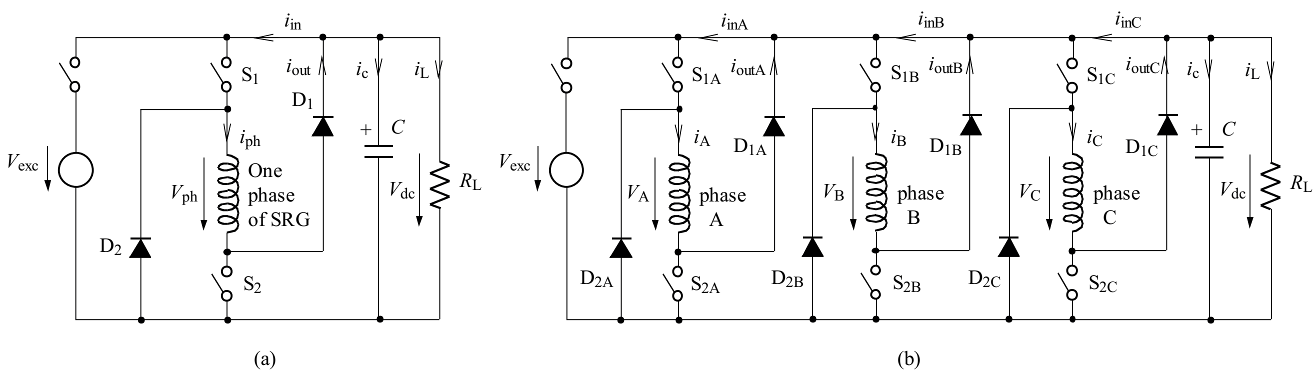

Fig. 3. Equivalent circuit of $2m$ converter in (a) – single phase, (b) – three phase operation

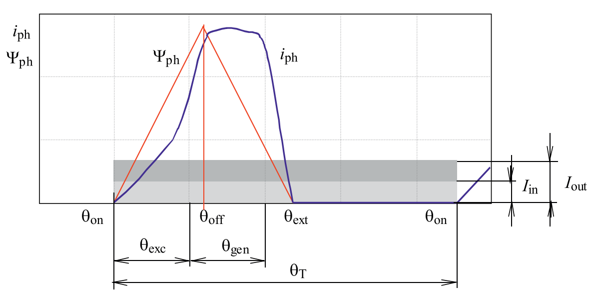

Fig. 4. Definition of the input and output currents

θ_{off} and P_{out} at $3\,000\,\mathrm{min}^{-1}$ and $v_{dc} = 300$ V. The output power was changed by the load resistance changing. It is seen that by a given output power, θ_{exc} and mainly I_{RMS} achieve their local minimum on a specific range of θ_{off} and this is important for design of converter VA rating. The local minimum of the θ_{exc} is at $\theta_{off} = 36 \div 40°$, the local minimum of the current is at the $\theta_{off} = 30 \div 34°$.

The block diagram for the multi-pulse operation differs from Fig. 5 only in the input parameters, where is also θ_{on}. The PI regulator comparing the required and real value of the voltage generates the required value of the current. The both switches are switching simultaneously on and off with hysteresis 2 A. Simulated waveforms of inductance, current, voltage, switch pulses and DC voltage gained by the converter $2m$, are in Fig. 8.

2.3 Converter with a neutral point of the source (Cnps)

In Fig. 9 there is a two-phase converter with a neutral point of the source (split DC supply converter-is its name for the motoring operation), which is suitable for SRG operation because it enables energy regeneration to the DC source. In fact, it is one switch per phase converter. This converter must have an odd phase number. Its advantage is its possibility of current overlapping and employing of the whole torque zones. Its disadvantage is that it is not possible to apply zero voltage, only either positive voltage from one capacitor, or negative from the other. It is controlled only by hard switching, what increases switching frequency and switching losses.

A complete mathematical model would consist of 14 equations for 5 voltages and 9 currents from the circuit in Fig. 9. Here only basic the differential equations for both phases are given.

$$\frac{\mathrm{d}i_a}{\mathrm{d}t} = \frac{1}{L_a}\Big[v_a - \Big(R_a + \frac{\mathrm{d}L_a}{\mathrm{d}\theta}\omega\Big)i_a\Big], \tag{12}$$

$$\frac{\mathrm{d}i_b}{\mathrm{d}t} = \frac{1}{L_b}\Big[v_b - \Big(R_b + \frac{\mathrm{d}L_b}{\mathrm{d}\theta}\omega\Big)i_b\Big] \tag{13}$$

with capacitors currents

$$i_{c1} = i_{D1} - i_{T1} - i_L\,, \tag{14}$$

$$i_{c2} = i_{D2} - i_{T2} - i_L\,, \tag{15}$$

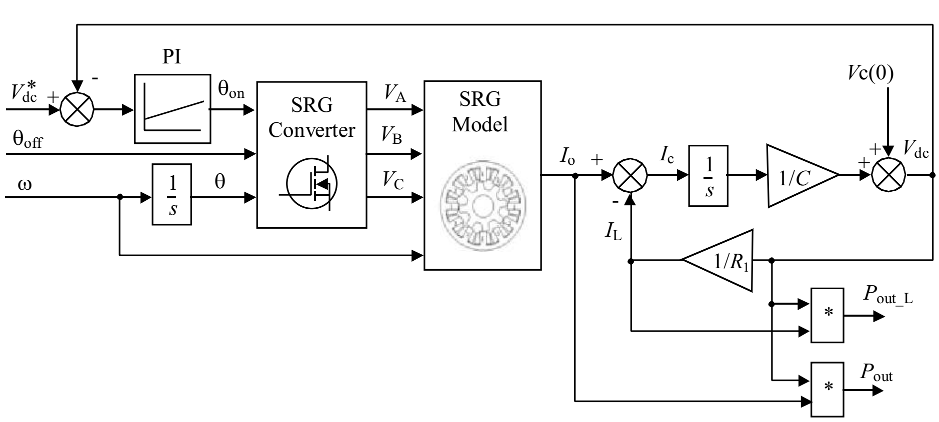

Fig. 5. Block diagram of the SRG model employed for one-pulse operation

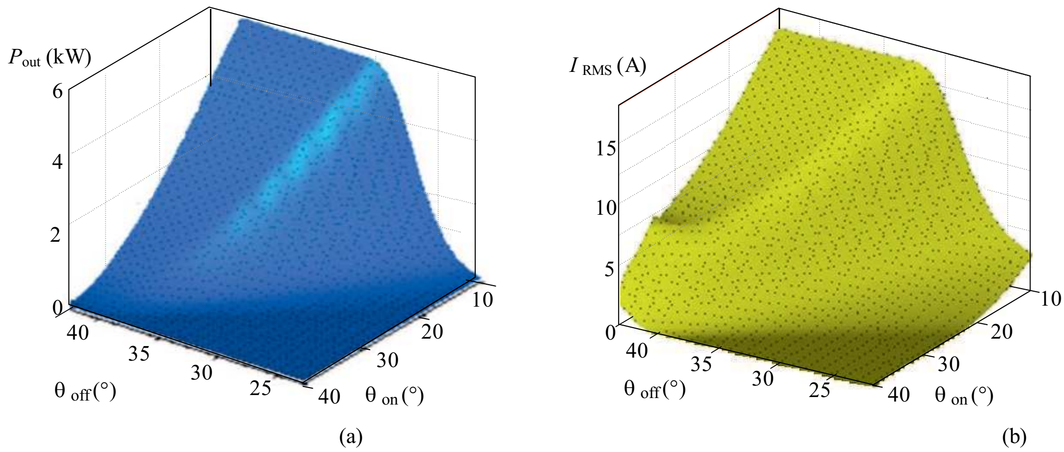

Fig. 6. (a) – power output and, (b) – phase current *vs* excitation parameters at 3 000 min^{-1} and $v_{\rm dc} = 300$ V

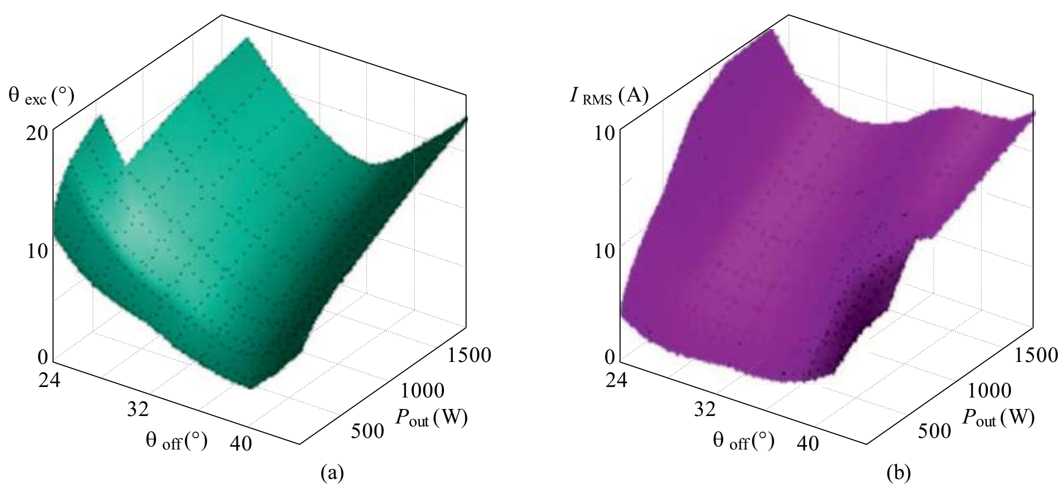

Fig. 7. (a)– excitation period, and (b) phase current *vs* $\theta_{\rm off}$ and $P_{\rm out}$ at 3 000 rpm and $v_{\rm dc} = 300$ V

where transistor current i_{T1}, (i_{T2}) is equal to the current of the corresponding phase if the transistor is switched on, otherwise is zero, diode current i_{D1} (i_{D2}) is zero if the transistor with the same symbol is switched on, otherwise is equal to the phase current. The voltages can be expressed as follows

$$v_a = \begin{cases} +v_{c1}\,, & \text{if } T1 \text{ is switched on,} \\ -v_{c2}\,, & \text{if } T1 \text{ is switched off and } i_a > 0\,, \\ 0\,, & \text{if } T1 \text{ is switched off, and } i_a = 0\,. \end{cases} \qquad (16)$$

$$v_b = \begin{cases} +v_{c2}\,, & \text{if } T2 \text{ is switched on,} \\ -v_{c1}\,, & \text{if } T2 \text{ is switched off and } i_b > 0\,, \\ 0\,, & \text{if } T2 \text{ is switched off, and } i_b = 0\,. \end{cases} \qquad (17)$$

The load current is determined by the voltage on the load and its resistance

$$I_L = \frac{v_{dc}}{R_L} \qquad (18)$$

where load voltage is given by the sum of the voltages of both capacitors

$$v_{dc} = v_{c1} + v_{c2}\,. \qquad (19)$$

To be able to compare the simulated values and important parameters with other converters, a four phase version will be introduced and analyzed. The capacitor $C1$ excites two phases (A and B) and accumulates the energy from the other two phases (C and D). The phases can be excited in A-C- B-D sequence or A-B-C-D, what is a case of the following simulations.

In Fig. 11 there are waveforms of four phase converter with neutral point of the source. Its further important performances will be compared with other kinds of converters below.

2.4 Converter with dump-capacitor (Cdc)

A model of a single phase converter with dump- capacitor C_d is in Fig. 12 and its complete mathematical model is as follows

$$\frac{{\rm d}i_a}{{\rm d}t} = \frac{1}{L_a}\Big[v_a - \Big(R_a + \frac{{\rm d}L_a}{{\rm d}\theta}\omega\Big)i_a\Big], \qquad (20)$$

$$i_{T1} = \begin{cases} i_a\,, & \text{if } T1 \text{ is switched on,} \\ 0\,, & \text{if } T1 \text{is switched off,} \end{cases} \qquad (21)$$

$$i_{D1} = \begin{cases} i_a\,, & \text{if } T1 \text{is switched off,} \\ 0\,, & \text{if } T1 \text{ is switched on,} \end{cases} \qquad (22)$$

$$v_{ph} = \begin{cases} +v_{dc}\,, & \text{if } T1 \text{ is switched on,} \\ -v_{dc} - v_{cd}\,, & \text{if } T1 \text{ is switched off, } i_a > 0\,, \\ 0\,, & \text{if } T1 \text{ is switched off, } i_a = 0\,. \end{cases} \qquad (23)$$

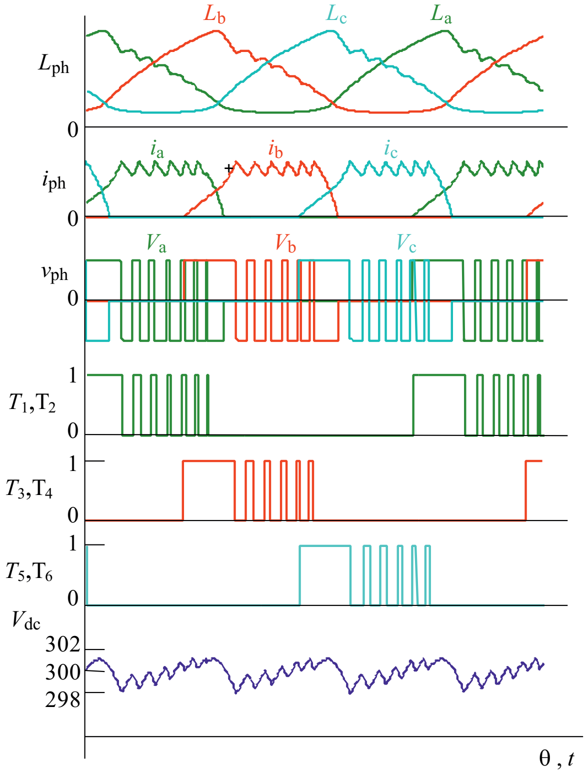

Fig. 8. Converter $2m$, simulated waveforms of the investigated three-phase SRG at 1000 rpm, $R_L = 2000\,\Omega$, $v_{DC} = 300$ V, $i^* = 10$ A, hysteresis control, hard switching

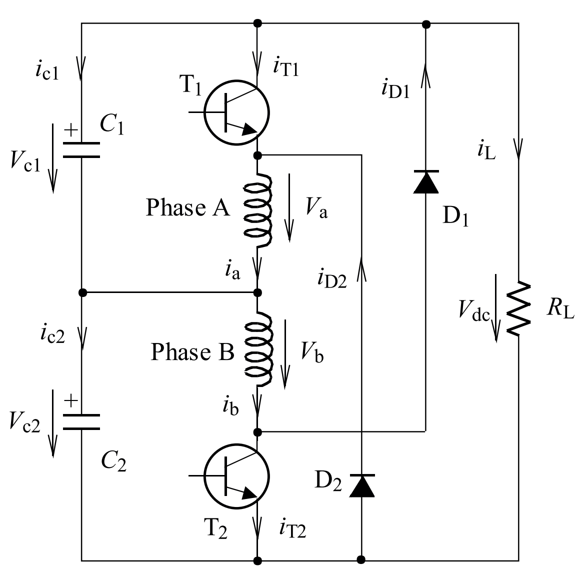

Fig. 9. Two-phase converter with a neutral point of the source

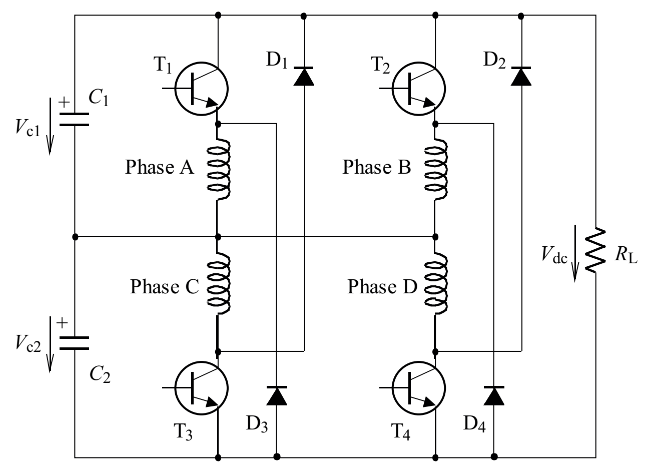

Fig. 10. Four phase version of the converter with neutral point of the source

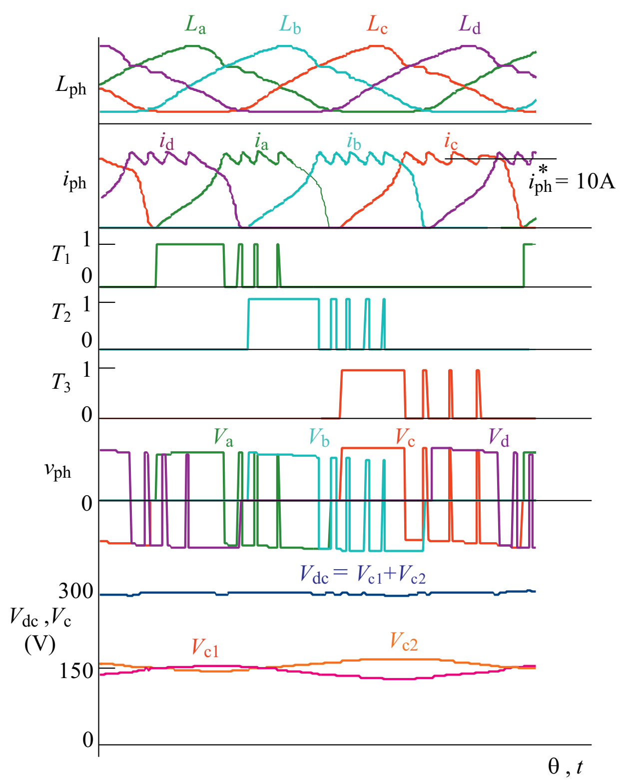

Fig. 11. Waveforms of four phase version of the converter with neutral point of the source at 1000 rpm, $R_L = 150\,\Omega$

A model for multiphase version would content four such equations for each phase. Further equations are current and voltages of capacitor C_d

$$i_{cd} = i_{D1} - i_{Tr}\,, \tag{24}$$

$$\frac{\mathrm{d}v_{cd}}{\mathrm{d}t} = \frac{i_{cd}}{C_d}\,. \tag{25}$$

And currents of elements of pulse converter

$$i_{Tr} = \begin{cases} i_{Lr}\,, & \text{if } T_r \text{ is switched on,} \\ 0\,, & \text{if } T_r \text{ is switched off,} \end{cases} \tag{26}$$

$$i_{Dr} = \begin{cases} i_{Lr}\,, & \text{if } T_r \text{is switched off,} \\ 0\,, & \text{if } T_r \text{ is switched on,} \end{cases} \tag{27}$$

$$\frac{\mathrm{d}i_{Lr}}{\mathrm{d}t} = \frac{v_{Lr}}{L_r} \tag{28}$$

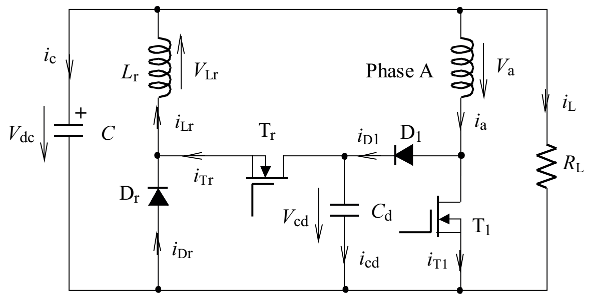

Fig. 12. Single phase version of the converter with capacitor

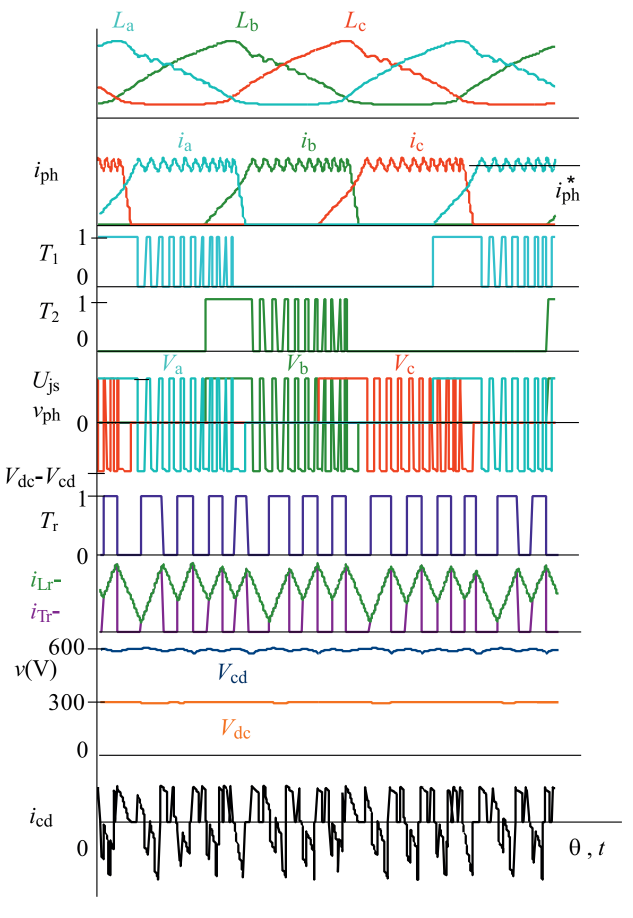

Fig. 13. Simulated waveforms of the important variables of the converter with capacitor

where

$$v_{Lr} = \begin{cases} +v_{cd} - v_{dc}\,, & \text{if } T_r \text{ is switched on,} \\ -v_{dc}\,, & T_r \text{ is switched off, } i_{Lr} > 0\,, \\ 0\,, & \text{otherwise.} \end{cases} \quad (29)$$

The last three equations describe capacitor current, load and DC voltage and are derived from Fig. 12.

$$i_c = i_{Lr} - i_a - i_L\,, \quad (30)$$

$$i_L = \frac{v_{dc}}{R_L}\,, \quad (31)$$

$$\frac{\mathrm{d}v_{dc}}{\mathrm{d}t} = \frac{i_c}{C}\,. \quad (32)$$

In Fig. 13 there are simulated waveforms of the important variables. It is seen that the currents are overlapped. The voltage has been controlled on the 600 V with hysteresis ±10 V, what is double of $v_{dc} = 300$ V.

A disadvantage of this converter is fact that the commutation of the currents depend on the difference between v_{dc} and v_{cd}. A fast commutation requires higher v_{cd} and hence higher voltage rating of semiconductor elements and capacitor C_d. Further, there are losses at the pulse converter and hence lower efficiency. This converter is not able to create zero voltage in the circuit therefore is possible to control it only with hard switching.

2.5 Converter for the SRG with bifilar winding (Cbw)

In Fig. 14 there is an equivalent circuit of the converter with bifilar winding.

A mathematical model must take into account that a ratio of the number of turns of both parts of the bifilar winding is in general "a". An equation for primary part of the bifilar winding (subscript "p")

$$\frac{\mathrm{d}i_{ap}}{\mathrm{d}t} = \frac{1}{L_{bif}}\Big[v_{ap} - \Big(R_{bp} + \frac{\mathrm{d}L_{bif}}{\mathrm{d}\theta}\omega\Big)i_{ap}\Big] \quad (33)$$

where L_{bif} is self-inductance of the primary part of the bifilar winding. In the equation for secondary winding (subscript "s") of the bifilar winding is taken into account that its phase inductance is inversely proportional to the a^2

$$\frac{\mathrm{d}i_{as}}{\mathrm{d}t} = \frac{a^2}{L_{bif}}\Big[v_{as} - \Big(R_{bs} + \frac{1}{a^2}\frac{\mathrm{d}L_{bif}}{\mathrm{d}\theta}\omega\Big)i_{as}\Big]\,. \quad (34)$$

Voltage equations are

$$v_{ap} = \begin{cases} v_{dc}\,, & \text{if } T_1 \text{is switched on,} \\ -av_{dc}\,, & \text{if } T_1 \text{is switched off and } i_{as} > 0\,, \\ 0\,, & \text{otherwise,} \end{cases} \quad (35)$$

$$v_{as} = \begin{cases} \frac{v_{dc}}{a}\,, & \text{if } T_1 \text{is switched on,} \\ -v_{dc}\,, & \text{if } T_1 \text{ is switched off and } i_{as} > 0\,, \\ 0\,, & \text{otherwise.} \end{cases} \quad (36)$$

The ratio of the number of turns of primary and secondary winding a has a significant influence on the current values in both parts of bifilar winding at the T_1 switching. If T_1 is switched on, i_{as} is zero, at the instant of the T_1 switching off, the value of i_{as} is changing from zero to the value of $i_{ap}a$, and at the instant of the T_1 switching on is changing to zero. If T_1 is switched off, the i_{ap} is zero and at the T_1 switching on is i_{ap} changing from zero to i_{as}/a and i_{as} is changing to zero (see Fig. 15). Then it can be written shortly:

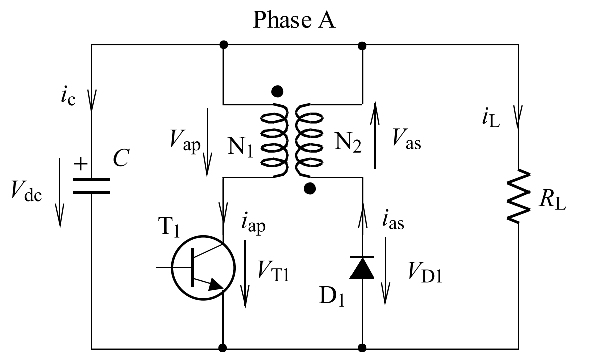

Fig. 14. Equivalent circuit of the converter with bifilar winding

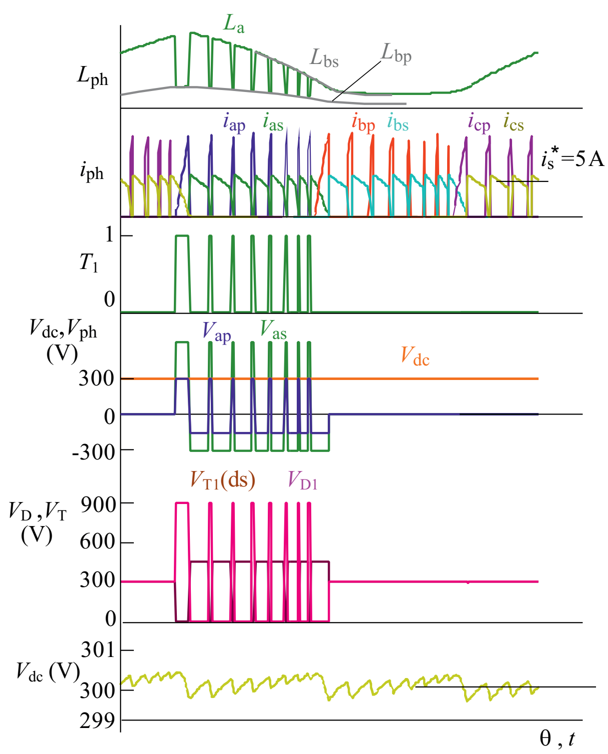

Fig. 15. Simulated waveforms of a three phase converter for SRG with bifilar winding

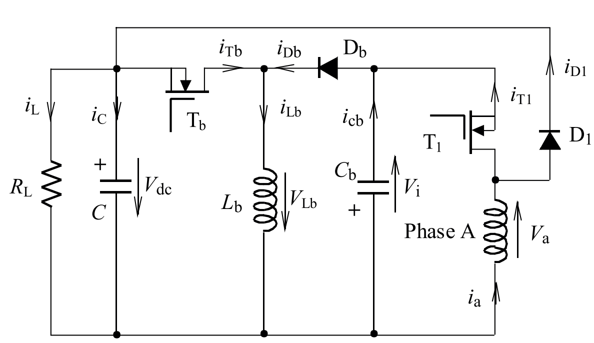

Fig. 16. Equivalent circuit of one phase of the converter with variable DC link

If T_1 is switched off, then $i_{as} = a\, i_{ap}$ and $i_{ap} = 0$.
If T_1 is switched on, then $i_{ap} = i_{as}/a$ and $i_{as} = 0$.

A capacitor current will be a difference between the currents of both parts of winding and load current

$$i_c = i_{as} - i_{ap} - i_L\,. \tag{37}$$

At the end, the equations for load current and DC voltage are as before

$$i_L = \frac{v_{dc}}{R_L}\,, \tag{38}$$

$$\frac{\mathrm{d}v_{dc}}{\mathrm{d}t} = \frac{1}{C} i_c\,. \tag{39}$$

In Fig. 15 there are simulated variables of the three phase SRG with bifilar winding, if the ratio of the turns number is $a = 0.5$. The DC voltage was kept at 300 V. The phase currents can be overlapped because this converter has no common switch and current control is independent. On the waveforms of the inductances is seen that self inductance of the primary winding L_{bp}, when T_1 is conducting is $\frac{1}{4}$ of the self inductance of the secondary winding L_{bs}, when D_1 is conducting. There is also seen that at the switching over T1 are currents and voltages always in the ratio of "a". Preferable is $a < 1$, because the primary winding is excited in very short time, what results in reduction of losses and excitation factor ε. On the other side there is a higher voltage loading of a diode and secondary winding.

2.6 Converter with variable DC link (CvDC)

In Fig. 16, there is a simplified equivalent circuit of one phase of a converter with variable DC link. The basic principles of operation can be explained on the base of this figure.

During an excitation T_1 is switched on, current flows through phase winding A, T_1 and C_b. Equations for currents i_{T1}, i_{D1} and a differential equation for the current i_{ph} are identical with (1), (2), (3) in Section 2.4. After a commutation of the $T1$ the current flows through the winding of the phase A, and D_1 and charges the capacitor C, therefore the voltage on the phase A can be

$$V_{ph} = \begin{cases} +v_i\,, & \text{if } T1 \text{ is switched on,} \\ -v_{dc}\,, & \text{if } T1 \text{ is switched off and } i_a > 0\,, \\ 0\,, & \text{if } T1 \text{is switched off, and } i_a = 0\,. \end{cases} \tag{40}$$

Equation for load current and voltage are again identical with Section 2.5, see (38) and (39).

Energy for repeated excitation is transmitted from capacitor C by means of switching T_b, therefore

$$i_c = i_{D1} - i_{Tb} - i_L\,, \tag{41}$$

where

$$I_{Tb} = \begin{cases} i_{Lb}\,, & \text{if } T_b \text{ is switched on,} \\ 0\,, & \text{if } T_b \text{ is switched off.} \end{cases} \tag{42}$$

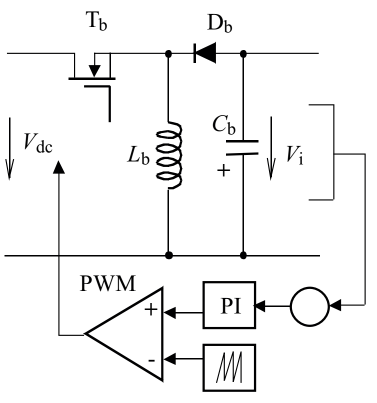

Fig. 17. Control of the converter with variable DC link

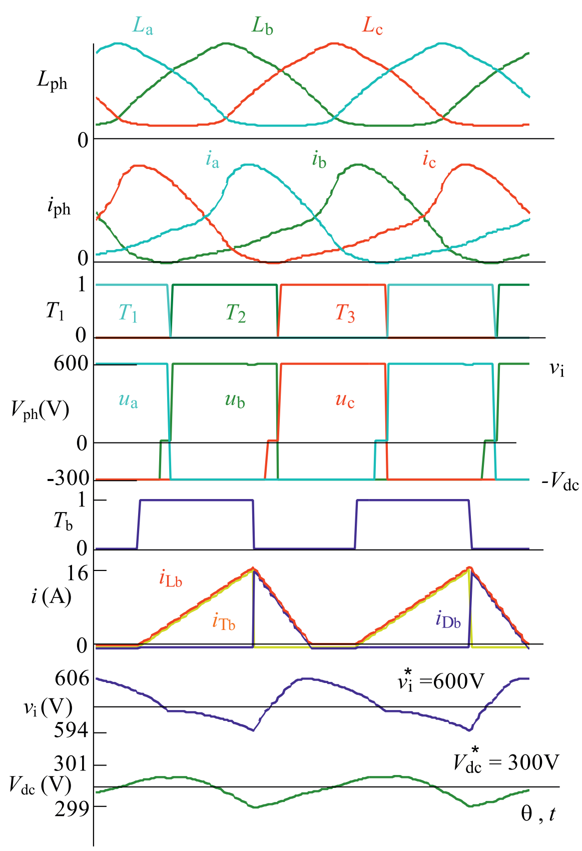

Fig. 18. Simulated waveforms of the three phase 12/8 SRG converter with variable DC link, $v_i = 2V_{dc} = 600$ V and $n = 10\,000$ rpm.

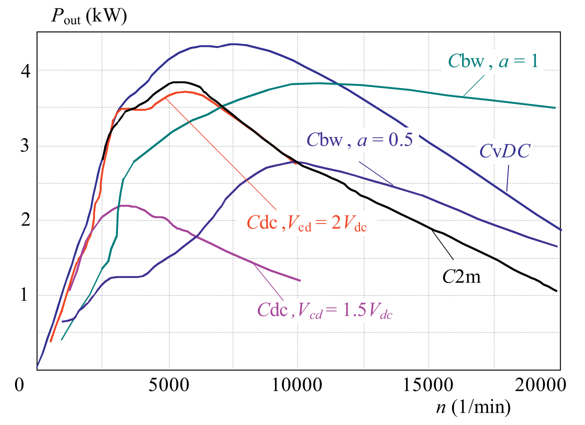

Fig. 19. Output power *vs* speed for investigated SRG converters

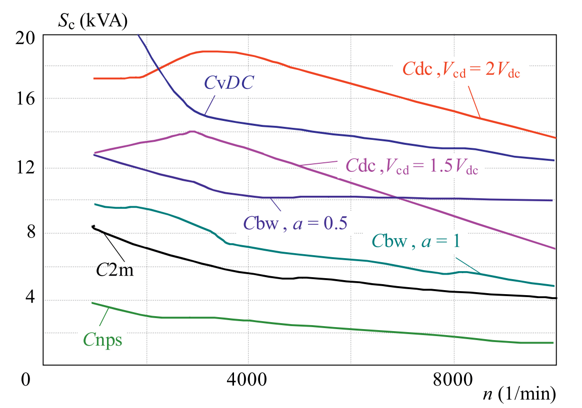

Fig. 20. Apparent power *vs* speed for investigated SRG converters

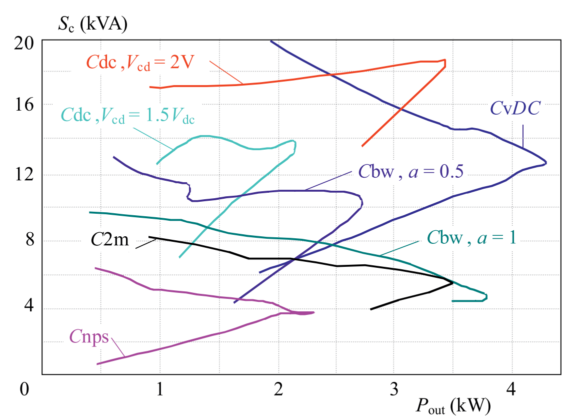

Fig. 21. Apparent power *vs* output power for investigated SRG converters

Energy is transmitted from DC circuit through the transistor T_b, inductance L_b to the capacitor C_b. The voltage and current of the L_b are as follows

$$v_{Lb} = \begin{cases} +v_{dc}\,, & \text{if } T_b \text{ is switched on,} \\ -v_i, & \text{if } T_b \text{ is switched off and } i_{Lb} > 0\,, \\ 0 & \text{otherwise,} \end{cases} \tag{43}$$

$$\frac{\mathrm{d}i_{Lb}}{\mathrm{d}t} = \frac{v_{Lb}}{L_b}\,. \tag{44}$$

The first derivation of the of the C_b voltage is directly proportional to its current

$$\frac{\mathrm{d}v_i}{\mathrm{d}t} = \frac{i_{Cb}}{C_b} \tag{45}$$

which is a sum of the currents through the inductance L_b, capacitor C, load and phase winding

$$i_{cb} = i_{Lb} - i_c - i_L - i_a\,, \tag{46}$$

Simulations have been carried out at the voltage $v_{dc} = 300$ V, as before. The transistor T_b of the pulse converter

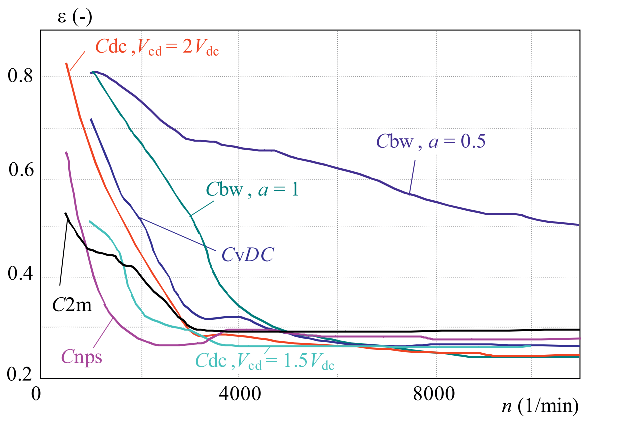

Fig. 22. Excitation factor *vs* speed for investigated SRG converters

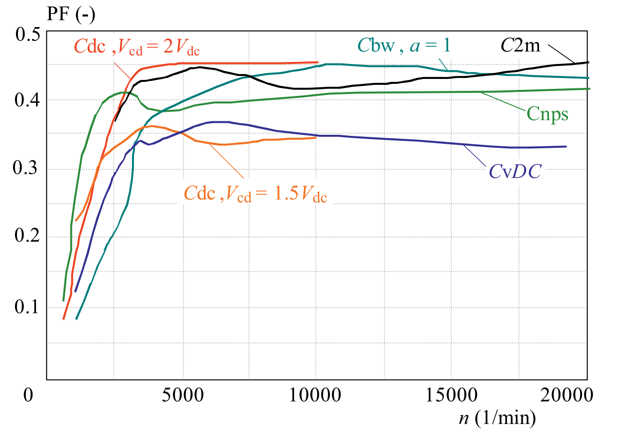

Fig. 23. Power factor *vs* speed for investigated SRG converters

Table 1. Comparison of the analyzed SRG converters

	Advantages	Disadvantages
Converter 2m (C2m)	– independent current conduction by $(+V_{dc}, 0, -V_{dc})$ – voltage stress of components $\Leftarrow V_{dc}$	– more switches
Converter with neutral point of the source (Cnps)	– less switches and diodes – voltage stress of components $\Leftarrow V_{dc}$ – independent control of phase currents	– phase is excited by lower voltage $(V_{dc}/2)$, but voltage stress of components $= V_{dc}$ – Suitable only for SRG with even number of phases – hard chopping only
Converter with dump capacitor (Cdc)	– less switches and diodes $(m+1)$ – possibility to generate the power by various voltage $(V_{ph} <> V_{dc})$	– higher voltage stress of components (commonly $2V_{dc}$) – additional losses on the pulse converter elements – voltage Vdc must be controlled independently from V_{cd} – hard chopping only
Converter with bifilar bifilar winding (Cbw)	– less switches and diodes (m) – possibility of rapid excitation and slow generating by $a < 1$, advantage by higher speeds	– more complicated bifilar winding – higher voltage stress of switches and/or diodes – air gap should be as small as possible, otherwise magnetic linkage get worse – the both primary and secondary winding current is to be sensed – only hard chopping
Converter with variable DC link (CvDC)	- less switches and diodes (m+1) - possibility of excitation with higher voltage $(V_{ph} > V_{dc})$ advantage by higher speed – less apparent power of pulse converter in comparison with converter with dump capacitor	– additional losses on the pulse converter elements – voltage V_i must be controlled independently from V_{dc} – only hard chopping

has been controlled on the base of PWM modulation to the output voltage $v_i = 600$ V, to be able to see a difference to asymmetrical converter (Fig. 17). In Fig. 18 there are simulated waveforms for the investigated SRG at 10 000 rpm. The speed is higher than its rated speed 3 000 rpm to show its advantage in this speed region. It is seen that the phase is active during the whole period of the phase current. Because magnetic flux arises faster at the higher excitation voltage v_i, the ratio of the $\theta_{\text{gen}}/\theta_{\text{exc}}$ is approximately 2 and is identical with the ratio of the v_i/v_{dc}.

3 THE COMPARISON OF THE ANALYSED SRG CONVERTERS

A comparison can be made in a table (see Table. 1) or in graphs (see Figs. 19–23).

In Fig. 19 there is output power *vs* speed for investigated SRG converters, in Fig. 20 apparent power *vs* speed, in Fig. 21 apparent power *vs* output power, in Fig. 22 excitation factor *vs* speed and in Fig. 23 power factor *vs* speed.

As it is seen in Fig. 19 the output power increases linearly up to the base speed what is around 3 000 rpm. This is in coincidence with the theory of operation on the constant torque and constant power. Then the SRG is in single-pulse operation where the region of constant power is quite narrow and the output power decreases with the speed.

In Figs. 20 and 21 there is apparent power *vs* speed and *vs* output power, respectively. At the first one there is seen that the apparent power decreases with the speed but there are big differences between particular topologies. The higher power is required at the topologies where only one common switch transmits energy, excited or generated one, or if its voltage is higher than v_{dc}. The higher apparent power is caused also by multi-pulse operation because it increases effective current through switches. At the second one there is apparent power vs. active power. As it is known, the better is lower ratio of the S/P_{out}. Therefore more suitable converters have their curves on the right side on the bottom. The most unsuitable converter is that with a capacitor, the power of which is 2 times more than that of $2m$ converter. The converter with variable DC link is suitable for increasing of the power at speed higher than base one. If the active power is increased by some tens of percent, the apparent power is increased by many times more because of higher voltage loading of the switches.

In Fig. 22 there is a factor of excitation ε, which expresses the reactive power in the circuit of SRG. Therefore it will have a big influence on the winding losses. The higher ε, the higher magnetizing power is needed for a phase to be able to get the same output power. This definition is generalized for all converters, also for those which have different voltage during excitation V_{exc} and during generation V_{gen}. Then the factor will be defined as follows

$$\varepsilon = \frac{I_{in}V_{exc}}{I_{out}V_{gen}}. \qquad (47)$$

In Fig. 22 there is seen that ε decreases with the speed and in one-pulse operation has the values around 0.26 till 0.3 (it is not true for the converter with the lower number of switches than $2m$, because there exist mutual influence between the currents). The values of ε in single-pulse operation in fact do not depend on the kind of converter, only on the geometrical dimensions of the SRG, such as air gap, material of the magnetic system, and inductance ratio.

In Fig. 23 there is power factor *vs* speed for investigated SRG converters. The power factor (PF) is evaluated on the base of the next expression

$$PF = \frac{P_{out}}{mV_{rms}I_{rms}}. \qquad (48)$$

It is seen that the PF approaches the values of 0.45.

4 A CHOICE OF THE SUITABLE CONVERTER TOPOLOGY

On the base of findings given in this paper some recommendation can be made for the choice of suitable SRG converter topology. Criterion for the choice could be: output power, speed, price of the converter (according the apparent power), or efficiency of the operation (according the PF). The classical $2m$ converter is most suitable for the lower speed till the base speed with regard to the power and efficiency. If the phase number is even, it would be enough also the converter with neutral point of the source.

For the high power at the speed above the base one, it is suitable to employ the converter with variable DC link, at the price of increasing of apparent power and decreasing of efficiency by adding some other elements. If the speed is some multiple of the base speed, the converter with bifilar winding is more suitable. But this converter is more demanding for the manufacturing because it requires a high quality of a magnetic link between the primary and secondary windings.

The converter with variable DC link has an advantage in comparison with the $2m$ converter because its electromotive force (induced voltage v_i) can be adjusted with speed what enables to adjust the output power. The power is at the constant speed directly proportional to the torque and this is proportional to the magnitude of magnetic flux linkage ψ. This magnitude is proportional to v_i and the instant of switch on, it means at the constant speed to the θ_{exc}.

In Fig. 24 there is seen magnetic flux linkage of the converter with variable DC link at $v_i = v_{dc}\,(\psi_1)$, and $v_i = 2V_{dc}\,(\psi_2)$.

In Fig. 25a there is comparison of simulated energy conversion loops of the three phase $2m$ converter and converter with variable DC link at $V_{\text{dc}} = 300$ V, $I_{\text{rms}} \le 10$ A, and $v_i = 2V_{\text{dc}}$ and $v_i = 3V_{\text{dc}}$. At each curve is put also the output power. It is seen that at 10 000 rpm the power does not increase very much if v_i changes from $2V_{\text{dc}}$ to $3V_{\text{dc}}$ because the current was limited to 10 A. But the apparent power has been increased by 30.7 %. In Fig. 25b, at the 20 000 rpm the power has been increased by 23.3 % and apparent power by the 57 %. The conclusion is that it is not suitable to increase the v_i to the higher value because the apparent power is enormously increased.

5 CONCLUSION

On the base of the analysis and discussions made in this chapter it can be observed that most favorite is $2m$ converter ($C2m$), because it has universal advantage from the point of view of output power, efficiency, phase number and controllability and has not very distinctive disadvantage.

On the other hand it can be concluded that it is not very suitable to employ the converter with capacitor, because it has very high apparent power. This kind of converter is very favorable at motoring operation at high speeds, at which its advantage is the controllable phase voltage at the decay of phase current (at regeneration).

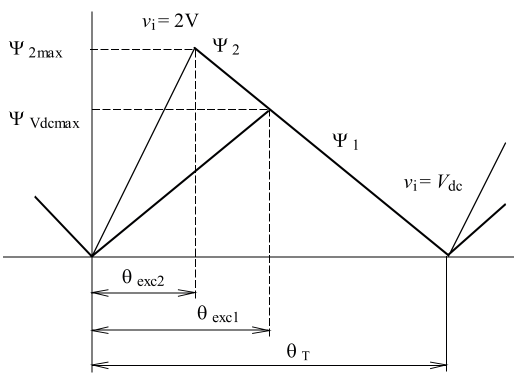

Fig. 24. Waveforms of linkage magnetic flux of the SRG with converter with variable DC link at $v_i = v_{dc}\,(\psi_1)$, and $v_i = 2v_{dc}(\psi_2)$

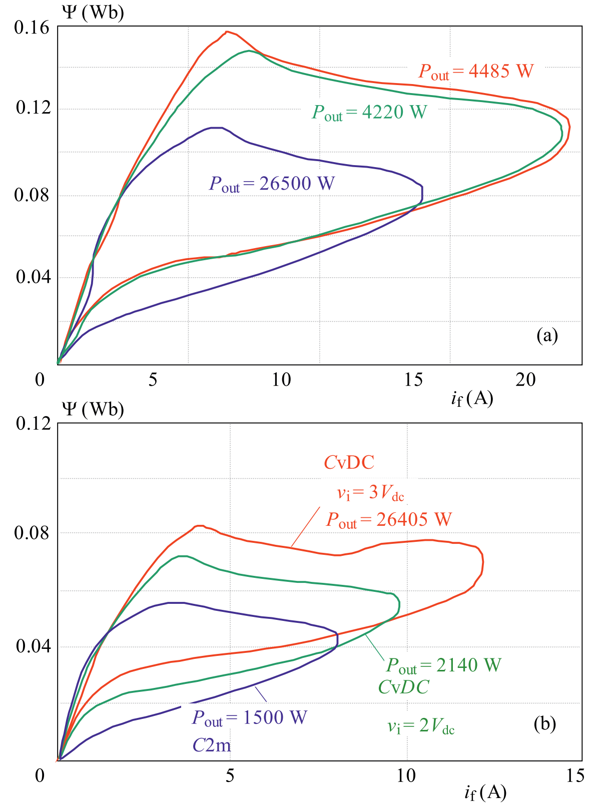

Fig. 25. Energy conversion loops of the SRG with $2m$ converter and converter with variable DC link a) – 10 000 rpm, b) – 20 000 rpm

Acknowledgements

This work was supported by R&D operational program Centre of excellence of power electronics systems and materials for their components No. ITMS II-2622012003 and by the Slovak Research and Development Agency under the Contract No. SK-RO-0028-12.

References

[1] MILLER, T. J. E.—: Electronic Control of Switched Reluctance Machine, Newnes Power Engineering Series, Oxford, GB, 2001.

[2] KRISHNAN, R.: Switched Reluctance Motor Drives – Modeling, Simulation, Analysis, Design, and Applications, CRC Press LLC, FLA, USA, 2000.

[3] DESHPANDE, V. V.—YOUNG LIM, J.: New Converter Configurations for Switched Reluctance Motors wherein some Windings Operate on Recovered Energy, IEEE Transactions on Industry Applications **38,** No. 6 (Nov-Dec 2002).

[4] CHEN, H.—ZHU, Y.—ZHANG, D.: Design of the Power Converter for 600 kW Switched Reluctance Motor Drive, Power Electronics Specialists Conference, 2002, vol. 4, 23-27 June 2002, pp. 1913–1918.

[5] LIPTÁK, M.—HRABOVCOVÁ, V.—RAFAJDUS, P.—ZIGMUND, B.: Switched Reluctance Machine with Asymmetric Power Converter in Generating Mode, Acta Electrotechnica et Informatica, Košice, 1/2007.

[6] RAFAJDUS, P.—HRABOVCOVÁ, V.—HUDÁK, P.: Investigation of Losses and Efficiency in Switched Reluctance Motor, 12th Internation Power Electronics and Motion Control Conference, EPE-PEMC 2006, Portorož, Slovenia, 2006 08, p.: T4-309.

[7] LIPTÁK, M.—HRABOVCOVÁ, V.—RAFAJDUS, P.: Equivalent Circuit of Switched Reluctance Generator Based on DC Series Generator, J. Electrical Engineering **59** No. 1 (2008), 23–28.

[8] TORREY, D. A.: Switched Reluctance Generators and their Control, IEEE Trans. on Industrial Electronics **49** No. 1 (Feb 2002), 3–14.

[9] SILVENTOINEN, P.—SALO, J.—TOLSA, K.—PYRHÖNEN, J.: Dynamic Tests with a Switched Reluctance Motor Drive, IEEE AES Systems Magazine (Jan 1999,), 25–28.

Received 3 July 2012

Valéria Hrabovcová graduated in electrical engineering from the University of Žilina and gained her PhD in electrical engineering from Slovak University of Technology in Bratislava in 1985. She is a professor of electrical machines at University of Žilina, Faculty of Electrical Engineering. Her professional and research interests include classical, permanent magnets and electronically commutated electrical machines.

Pavol Rafajdus was born in Trnava, Slovakia, in 1971. He received the MSc and PhD degree in electrical engineering from University of Žilina, Slovakia, in 1995 and 2002, respectively. At present he is an associate professor at the Faculty of Electrical Engineering, University of Žilina. His research is focused on the electrical machines, mainly switched reluctance motors and other electrical machine properties.

Martin Lipták (MSc, PhD) received his MSc degree in Electrical engineering from the University of Žilina in 2002. Between 2002 and 2005 he was a PhD student at the University of Žilina. Currently he is with Treves s.r.o., Czech Republic

Loránd Szabó was born 1960 in Oradea (Romania). He received the BSc and PhD degree from Technical University of Cluj (Romania) in electrical engineering in 1985 and 1985, respectively5. Currently, he is a professor in the Department of Electrical Machines of the same university. His research interests are in the areas of variable reluctance machines, fault detection, *etc.* He published over 170 scientific papers and books in these fields.